Improving gear shift quality in a PHEV DCT with integrated PMSM

Muddassar Zahid Piracha
Industrial PhD Student, Electric Propulsion Systems
CEVT AB, Sweden

Dr. Anders Grauers
Associate Professor, Hybrid and Electric Vehicle Systems
Chalmers University of Technology, Sweden

Johan Hellsing
Technical Specialist, Electric Propulsion Systems
CEVT AB, Sweden

ABSTRACT

In this paper a hybridized Dual Clutch Transmission (DCT) is presented in which a traction Permanent Magnet Synchronous Motor (PMSM) is mounted on the input side of the even gears. As the motor has high power, it has a high inertia. This leads to increased shift time in Electric Vehicle mode (EV mode). In EV mode, ICE is shut down and both clutches are open and vehicle is driven by PMSM on even gears. Since both off going and oncoming gears are on the same shaft, there will be a torque interrupt during shifts in EV mode.

The main focus of this paper is the speed synchronization phase during torque interrupt shifts. Currently the speed synchronization is done by using PMSM only. This sometimes leads to slower shift times and a degraded drivability due to battery power limitations. The speed synchronization can also not be achieved by synchronizers alone as is done in traditional DCTs due to added inertia of PMSM.

This paper explains the detailed modeling of synchronizers for simulating speed synchronization times during torque interrupt shifts. The PMSM model is based on a loss map and inertia. The effects of the available power from the battery on speed synchronization are also modelled. A high level modeling is done for rest of the powertrain. Based on simulations, first the increased synchronization time and its main limiting factors are discussed. A prediction model is also developed which, before a shift is ordered by high level strategy, creates the speed synchronization trajectories for PMSM and synchronizer. Based on prediction model, a high level supervisory control strategy is developed that will communicate between synchronizer and motor controller to ensure minimum synchronization time based on the limitations in synchronizer and battery.

The study can be extended to general treatment of clutchless multi-speed transmissions in electric vehicles and their effects on shift quality in general.

1 Background

This paper analyses a hybrid 7 speed DCT (7DCTH) in a parallel hybrid electric vehicle (PHEV) application as shown in Figure 1. There are several methods to hybridize a traditional DCT but the method shown has two major advantages over other methods

1. Involves minor platform changes
2. Clutch 1 and 2 must be designed for torque of ICE only

Since it is a PHEV application the vehicle spends significant percentage of driving time in EV mode

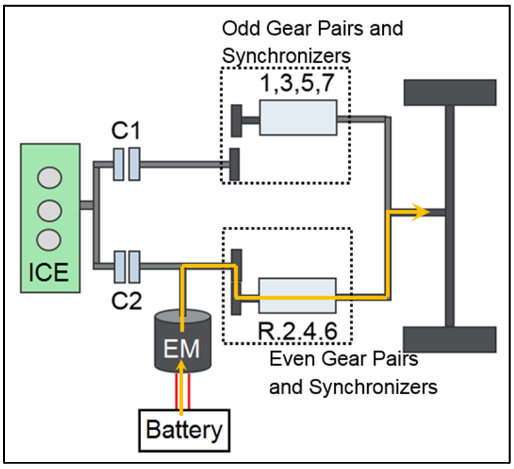

Figure 1 Layout of 7DCTH and its EV mode

The operation in EV mode is shown in Figure 1, when both clutches C1 and C2 are open and the combustion engine is off. The electric motor (EM) will be driving the vehicle via even gears as shown by the yellow line representing the power flow.

2 Torque Interrupt shift

Based on power flow shown in Figure 1, the 7DCTH in EV mode can be seen as equivalent to a manual transmission as shown in Figure 2.

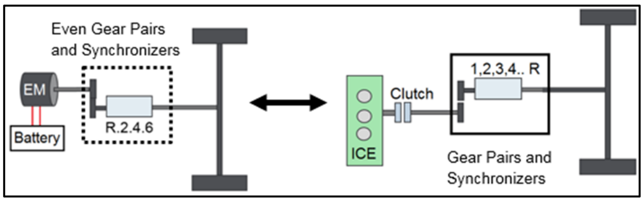

Figure 2 EV mode as a manual transmission

In a manual transmission the shifts are always torque interrupt shifts so in the 7DCTH in EV mode the shifts will also be torque interrupt shifts. A torque interrupt shift has the following phases.

1. Torque ramp down
2. Sleeve to Neutral
3. Speed Synchronization
4. Sleeve to Gear
5. Torque Ramp up

The shift time for a torque interrupt shift is defined as time from when the torque starts ramping down to time when the torque has fully ramped up. Shift time is an important factor in drivability since during this time the driver does not get the requested torque and unwanted changes in acceleration are felt by the driver. In order to maintain drivability the shift time must be minimized.

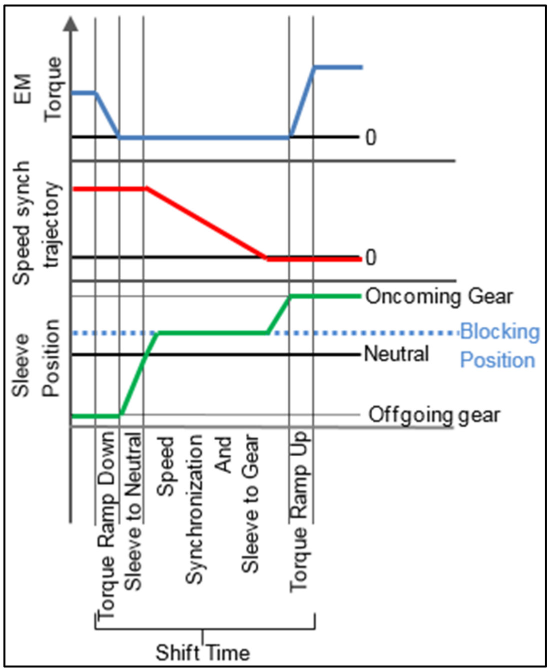

Figure 3 Torque interrupt shift phases with Speed Synchronization using synchronizer

The largest percentage of torque interrupt time is spent in Speed Synchronization, i.e. matching the speed of oncoming idler to the shaft or sleeve/hub velocity of synchronizer. In a 7DCTH this speed synchronization can be done by one of following 3 ways

1. Using only synchronizer as is done in a Manual transmission or a traditional DCT
2. Using only electric motor as is done in electric drives having dog clutches
3. Using first electric motor and then synchronizer

2.1 Using Synchronizer only

The shift phases when speed synchronization is done only using synchronizer are shown in Figure 3.

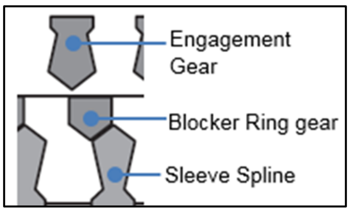

Figure 4 Sleeve at Blocking Position [3]

The electric motor is turned off during the speed synchronization phase. The sleeve will stay at blocking position until the speed difference is zero as shown in Figure 4 and denoted by blue dotted line in Figure 3.

Since inertia that needs to be synchronized in 7DCTH includes the high electric motor inertia, it means synchronization time will be longer. For manual transmissions and traditional DCTs the inertia that needs to be synchronized only includes shaft inertias which means that speed synchronization can be done in reasonable times with only the synchronizer.

2.2 Using Electric motor only

If speed synchronization is done by using electric motor only the shift phases are shown in Figure 5. In this case, the synchronizer is moved from neutral once the electric motor has made the speed difference zero. This approach is implemented today and works for cases where enough battery power is available.

2.3 Using Both Electric motor and Synchronizer

If speed synchronization is done by synchronizer only, the contribution of electric motor is neglected and vice versa. So the proposed strategy in this paper is to first use electric motor and then synchronizer, to minimize the shift time, if the available power from battery is too low or if the synchronizer system is exceeding its limits in terms of frictional work for the lining of the friction material. The shift phases then would be as shown in Figure 6. This is essentially extending speed synchronization phase into part of sleeve engagement phase to decrease the overall speed synchronization time.

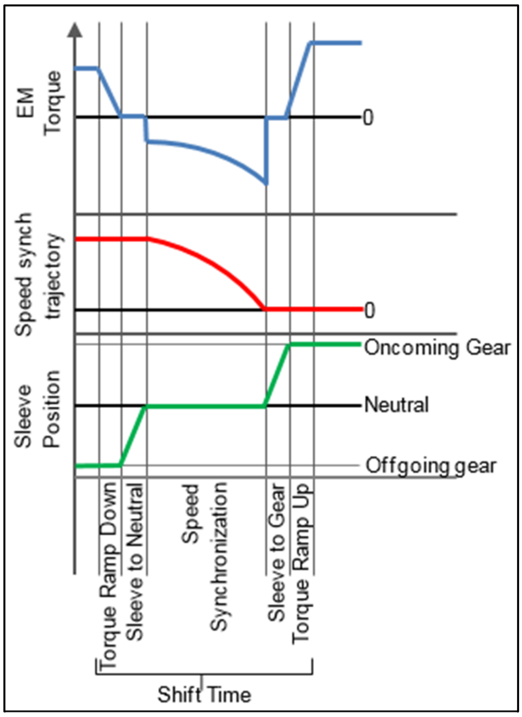

Figure 5 Torque interrupt shift phases with Speed Synchronization using electric motor

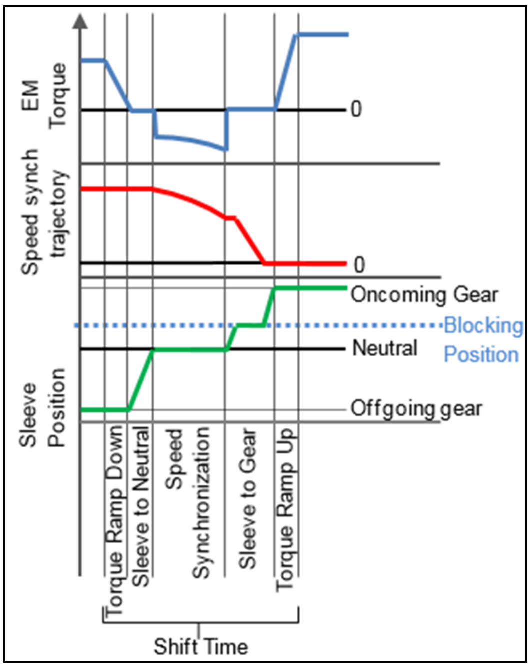

Figure 6 Speed Synchronization using electric motor and synchronizer

3 Calculation of speeds during shift

The speeds during shift are calculated based on the simple driveline model as shown in Figure 7. The angular velocity of drive shaft is

$$\omega_{drive\ shaft} = v_{veh} \div R_w \quad (1)$$

where v_{veh} is vehicle velocity at shift and R_w is the radius of wheel. Shift velocity v_{shift} can be defined as vehicle speed at which a shift is ordered from high level controller. Shift velocity is calculated from ''shift maps'' and is based on accelerator pedal and initial gear.

The high level control also gives the target gear. Once the vehicle velocity is equal to shift velocity the current oncoming idler speed ω_g and the current sleeve speed ω_s can be calculated by

$$\omega_s = \omega_{side\ shaft} \times Final\ Drive\ Ratio \quad (2)$$

$$\omega_{output\ shaft} = \omega_s \tag{3}$$
$$\omega_{input\ shaft} = \omega_{output\ shaft} \times Initial\ Gear\ Ratio \tag{4}$$
$$\omega_g = \omega_{input\ shaft} \div Target\ Gear\ Ratio \tag{5}$$

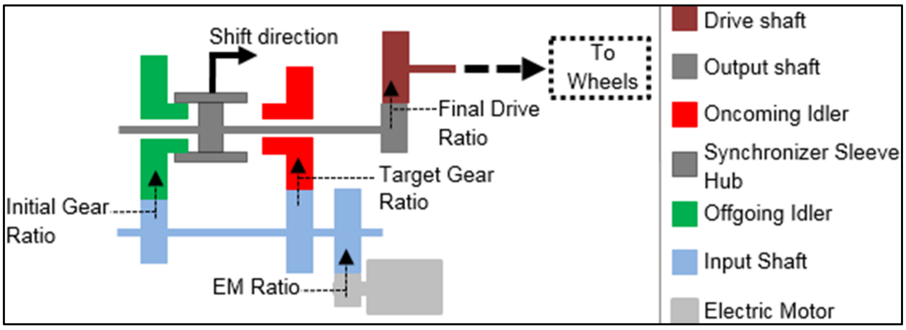

Figure 7 Speed relation between different components

The speed synchronization explained in section 2, is achieved when ω_g becomes equal to ω_s.
It is assumed that the vehicle velocity will remain constant during shift, which is a reasonable simplification since the vehicle does not have much time to decelerate if the shift is fast enough. Therefore it will not be a large difference between ω_s by equation 2 and real ω_s.
From Figure 7 the initial and final speed of electric motor ω_{em_i} and ω_{em_f} respectively can also be calculated by

$$\omega_{em\_i} = \omega_g \times Target\ Gear\ Ratio \times EM\ Ratio \tag{6}$$
$$\omega_{em\_f} = \omega_s \times Target\ Gear\ Ratio \times EM\ Ratio \tag{7}$$

4 Simulation model of Synchronizer

4.1 Gear Actuation Mechanism

A simplified model of gear actuation system is shown in Figure 8, showing the connection between gear shifter motor and synchronizer sleeve.

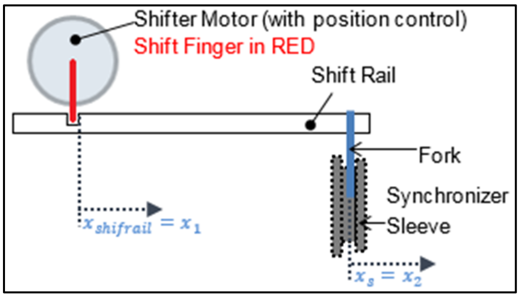

Figure 8 Gear actuation mechanism

The axial dynamics of sleeve can be written as

$$F_{ax} = k(x_2 - x_1) + d(\dot{x_2} - \dot{x_1}) \tag{8}$$

where F_{ax} is the force applied on sleeve, k is stiffness and d is damping of the complete mechanism.
In 7DCTH the shifter motor is position controlled so it gets the set point x_1 from high level control and the shifter motor applies a force F_{act} to make x_2 follow x_1. F_{ax} in terms of F_{act} can be written as

$$F_{act} = sat_{-F_{max}}^{F_{max}} \{F_{ax} + F_{pl}\} \tag{9}$$

where F_{pl} is the force from preload mechanism and is a function of sleeve displacement as shown in Figure 9. The

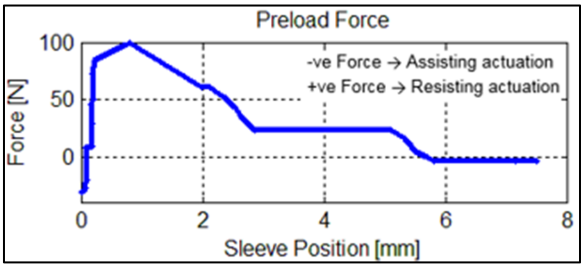

Figure 9 Preload force vs sleeve position

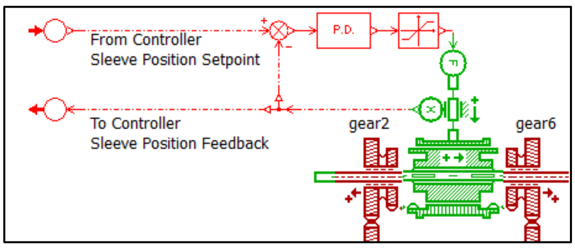

Figure 10 Position control implementation in AMESim

preload force calculation is done based on [1]. F_{max} is the maximum force of shifter motor. Equation 8 can be seen as the equation for a feedback PD controller i.e.

$$u = K_p e + K_d \dot{e} \tag{10}$$

Where u is the controller output, e and $\dot{e}$ is the error and its derivative respectively and K_p and K_d are the proportional and derivative gains and can be calculated by comparing equation 8 and equation 10.

The implementation of position control in AMESim is shown in Figure 10, with saturation block containing the shifter motor force limits in equation 9.

4.2 Simulation Model of synchronizer

The synchronizer is modeled as a state machine. The states and their corresponding equations are shown in Figure 11. As it can be seen in Figure 11 both longitudinal dynamics and rotational dynamics are included in the model. The conditions to leave the current state are written in black, the conditions to exit it are in red and the conditions to stay in the current state are in blue.

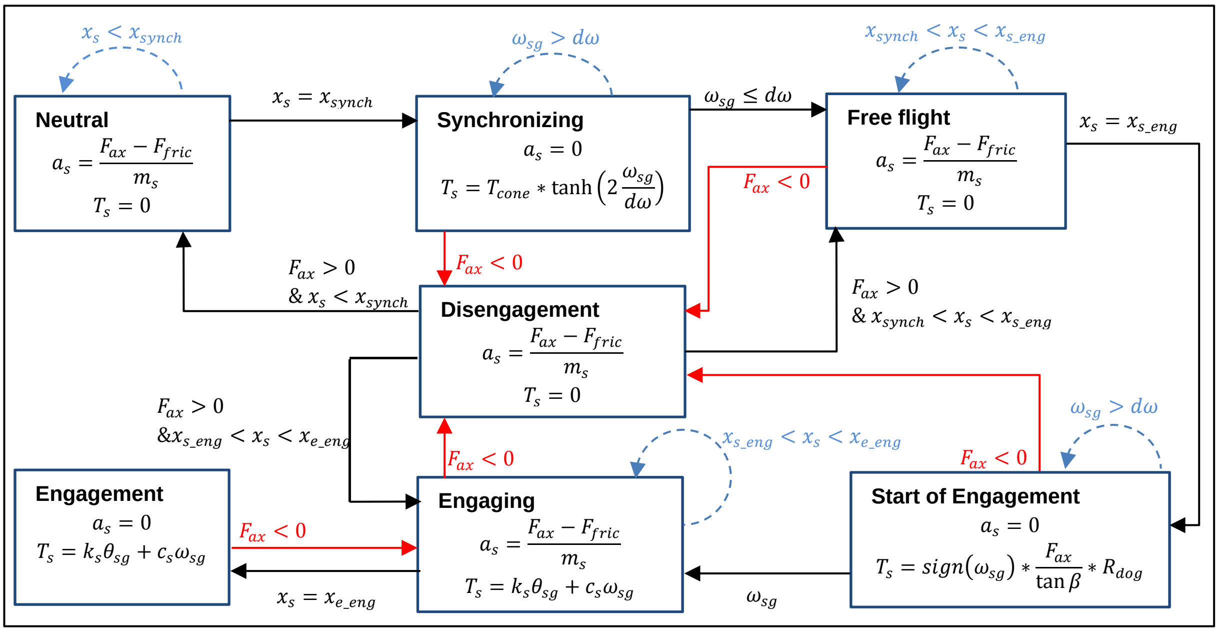

Figure 11 Simulation Model of synchronizer

where

a_s is acceleration of sleeve

m_s is mass of sleeve

x_s is displacement of sleeve, defined by tip of sleeve as shown by RED+ in Figure 12

x_{synch} is sleeve position, when synchronizing as shown in Figure 12

x_{s_eng} is sleeve position at start of engagement with idler gear teeth as shown in Figure 12

x_{e_eng} is sleeve position at end of engagement as shown in Figure 12

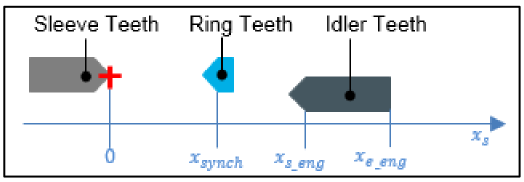

Figure 12 Sleeve position definition

T_s is torque applied on idler gear by sleeve

T_{cone} is clutch capacity of cone clutch as explained in section 4.3

ω_{sg} is relative velocity between sleeve and Oncoming idler gear and is described by

$$\omega_{sg} = \omega_s - \omega_g \tag{11}$$

$d\omega$ is relative velocity below which the cone clutch is assumed to be closed and is $\cong 0$
θ_{sg} is relative angular displacement between sleeve and gear
k_s is angular stiffness of sleeve teeth when engaged
c_s is angular damping of sleeve teeth when engaged
β is effective dog contact angle as shown in Figure 13
R_{dog} is effective radium of dog teeth as shown in Figure 13

4.3 Speed synchronization using synchronizer

As it can be seen in Figure 11 in ''Synchronizing'' state, sleeve will stay at blocking position $x_s = x_{synch}$ (as shown in Figure 4) until the velocity difference between sleeve and oncoming idler ω_{sg} is decreased to $d\omega \cong 0$.

The inertia J_{red} can be calculated as shown in [2] and to that adding the electric motor inertia. Note that the electric motor inertia need to be translated into an equivalent inertia as it is experienced by the idler gear by taking the EM gear ratio and target gear ratio into account. In this paper it is assumed that ω_{sg} will remain constant through ''Free flight'' state. Based on this assumption it can be stated that the ''Synchronizing'' state is where speed synchronization is done.

In the expression of sleeve torque T_s in the ''Synchronizing'' state, T_{cone} is the torque applied by cone clutch and the hyperbolic tangent function is an approximation used to correct its sign wrt ω_{sg} and give the model a smooth transition around $\omega_{sg} = 0$. A more exact modelling would be to use the sign function, however, since sign function is a discontinuity, it leads to smaller sampling times and consequently longer simulation time. T_{cone} is the maximum torque the clutch can produce with the available axial force and it can be calculated by

$$T_{cone} = n_c F_{ax} R \mu \div \sin\alpha \tag{12}$$

where n_c is the number of cones in synchronizer, R is the effective radius of ring cone, μ is friction coefficient of cone clutch and α is blocker ring cone angle as shown in Figure 13.

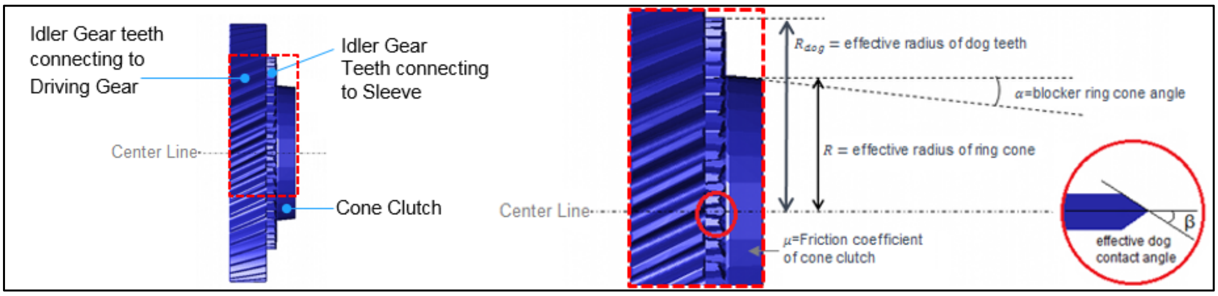

Figure 13 Idler Gear and Cone Clutch parameters

The angular acceleration of the idler, α_{Jred} when torque T_{cone} is applied will be

$$\alpha_{Jred} = (T_{cone} - T_d) \div J_{red} \tag{13}$$

From equation 13, the synchronization time t_s can be calculated by

$$t_s = \omega_{sg} \div \alpha_{Jred} \tag{14}$$

The heat generated by synchronization process is characterized by specific frictional work W_A of synchronizer as described in [2] and is

$$W_A = W \div A = 0.5 \times \left(J_{red}\omega_{sg}{}^2 + T_d \omega_{sg} t_s\right) \div A \tag{15}$$

Where W is frictional work and A is gross frictional surface area of synchronizer.

The specific frictional work during shifts must be kept below a certain limit W_{A_lim} in order to ensure the life of synchronizer. So

$$W_A < W_{A\_lim} \tag{16}$$

The inequality in equation 16 can be changed to an equality by choosing a safety factor

$$W_A = W_{A\_lim} \times (Safety\ Factor) \tag{17}$$

The safety factor for this paper is chosen to be 90% as advised by ''Product Design Specification''.

Now if W_A in equation 15 is such that the inequality in equation 16 is not satisfied, new values of relative velocity between sleeve and Oncoming idler gear ω_{sg_lim} and synchronization time t_{s_lim} need to be calculated, such that when ω_{sg_lim} and t_{s_lim} are used in equation 15 (as shown in equation 18) instead of ω_{sg} and t_s respectively, inequality in equation 16 is satisfied.

$$\mathrm{W_A} = 0.5 \times \left(J_{red}\omega_{sg\_lim}{}^2 + T_d\omega_{sg\_lim}t_{s\_lim}\right) \div A \tag{18}$$

The relation between $\omega_{sg\_lim}, t_{s\_lim}, \omega_{sg}, t_s,\ \omega_s$ and ω_g is shown in Figure 14.

Equation 9 can be rewritten for ω_{sg_lim} and t_{s_lim}, as

$$t_{s\_lim} = \omega_{sg\_lim} \div \alpha_{Jred} \tag{19}$$

Substituting the value of t_{s_lim} in equation 18, equation 18 can be solved for ω_{sg_lim} by using equation 17. The equation for ω_{sg_lim} is then

$$\omega_{sg\_lim} = \sqrt{(A * W_{A\_lim}(0.9)) \div 0.5(J_{red} + (T_d \div \alpha_{Jred}))} \tag{20}$$

Using equation 11, ω_{g_lim} can be calculated by

$$\omega_{g\_lim} = \omega_s - sign\left(\alpha_{Jred}\right) * \omega_{sg\_lim} \tag{21}$$

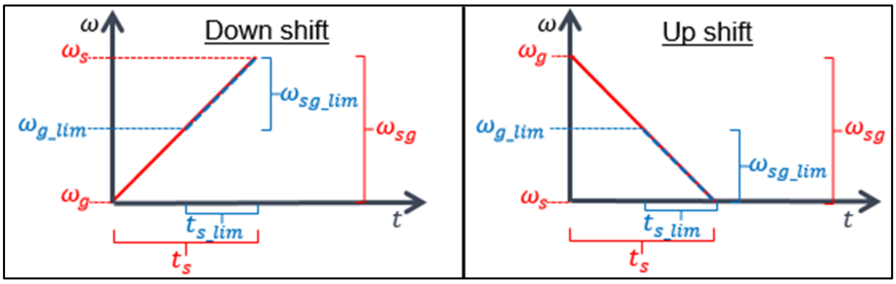

Figure 14 Allowed oncoming idler speed and allowed slip time during upshift and downshift

4.4 Prediction of speed synchronization trajectory with synchronizer

Equations 1 through 5 can generate ω_s and ω_g, for any shift velocity, before the vehicle has reached that velocity. Then using equations 11 through 14, t_s can be calculated to see the duration of speed synchronization if done using synchronizer only.

If the inequality in 16 is satisfied by the results of equation 11 and 14, then the shift will have negligible effect on the life of synchronizer.

If the inequality in equation 16, is not satisfied, then equations 21 and 19 give the value of limited oncoming idler speed ω_{g_lim} and limited synchronization time t_{s_lim} such that inequality in equation 16, is satisfied with respect to $Safety\ Factor$ in equation 17.

The oncoming idler and sleeve velocities can be translated to electric motor shaft speed using equations 6 and 7 respectively. The limited oncoming idler velocity can be translated using ω_{g_lim} as input in equation 6 as shown in equation below

$$\omega_{em\_iSL} = \omega_{g\_lim} \times Target\ Gear\ Ratio \times EM\ Ratio \tag{22}$$

Resulting ω_{em_i}, ω_{em_f} and ω_{em_iSL} from equations 6,7 and 21, when combined with values of t_s and t_{s_lim} from equation 14 and 19, result in representing the speed synchronization trajectory during shift at electric motor shaft in advance of the shift.

In essence it will be the same plot as Figure 14 but at electric motor shaft instead of on coming idler. In order to compare speed synchronization times between different shifts, synchronization times can be normalized wrt a typical speed synchronization time for a DCT. Electric motor shaft rpm vs normalized time, for two particular shifts is shown in Figure 15.

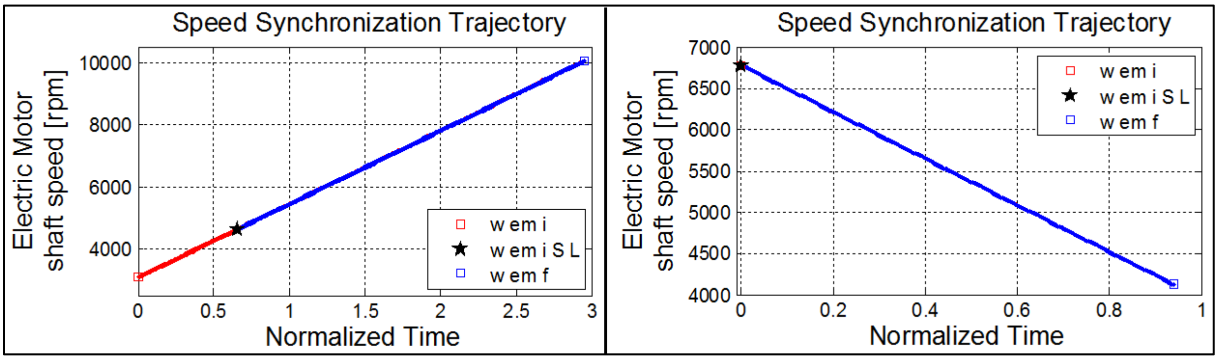

Figure 15 Speed synchronization trajectory for 6-2 Downshift (left) and 4-6 Upshift (right) using Synchronizer only

In Figure 15, in the left plot a 6-2 down shift with accelerator pedal fully pressed is shown, it can be seen that for this particular shift ω_{sg} will be such that the inequality in equation 16, will be not fulfilled so ω_{em_iSL} needs to be calculated and is denoted by star. This result means that the speed of the electric machine has to be increased to at least 4634 rpm before the synchronizer can be activated.
In Figure 15, in the right plot a 4-6 up shift with accelerator pedal fully pressed is shown, it can be seen that for this particular shift ω_{sg} will be such that the inequality in equation 16 will be satisfied so ω_{em_iSL} is equal to ω_{em_i}. In this case, the shift can be made with the synchronizer without exceeding its specific frictional work limit.

5 Simulation model of electric motor

5.1 Available Battery power

The battery power available during shift is characterized by pulse power of the battery defined by the power the battery can deliver for approximately 0.5 to 1 second.
If current is constant it implies plot of Power vs State of Charge (SOC) and plot of V_{OCV} have same shape as shown in Figure 16.

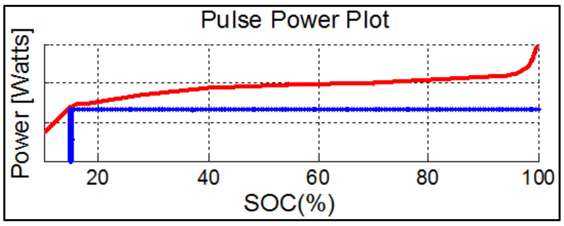

Figure 16 For constant current, Pulse Power vs SOC

Pulse power of the battery changes with SOC but it is made independent of SOC by keeping it constant at its value at SOC=15% as shown in Figure 16. In general

$Available\ Pulse\ Power\ of\ Battery \propto {}^{1}/_{Temperature}.$

At nominal operating conditions the pulse power available is as high as 40 kW, while at low temperatures and for aged batteries it is as low as 5 kW.
Pulse power available in the battery is an output from battery management software which is updated wrt to temperature conditions constantly.

5.2 Torque at a particular speed from electric motor

The torque electric motor can provide during shift depends on the battery power available and losses in the motor. In this study the losses in power electronics are neglected since they are small compared to motor losses but they can be very easily added in the algorithm. The motor losses are taken from measurements at the conditions with highest losses i.e. highest operating voltage and highest magnet temperature. The maximum and minimum electric motor torque available for downshift and upshift respectively is calculated from the algorithm shown in Figure 17.

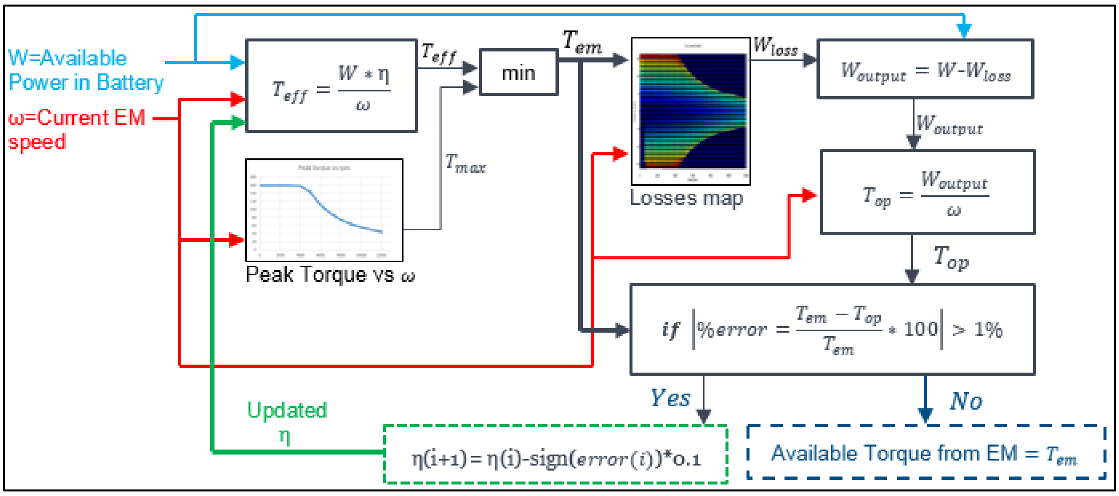

Figure 17 Calculation of Torque based on speed and battery power

As shown in Figure 17, a maximum torque T_{em} is calculated based on an initial guess of efficiency. Then T_{em} and current motor speed is used to find corresponding losses W_{loss} from the look up table. Based on W_{loss}, input battery power and current motor speed, a torque based on output power T_{op} is calculated. If the W_{loss} is the correct loss value then T_{em} will be equal to T_{op}.

If the value of T_{em} is not equal to the calculated T_{op} it means the initial guess of efficiency η was wrong. Then η is updated with the update law shown in the green dotted square in Figure 17. Value of η is updated until the absolute percentage error between T_{em} and T_{op} is less than 1%.

The working of the algorithm can be demonstrated by a simple test case. Suppose the torque motor can give at 3800 rpm when battery power is 5 kW is required. The initial guess of efficiency is 92%. The convergence of percentage error and efficiency is shown in Table 1.

Table 1 Example of Torque calculation algorithm

Iteration #	Efficiency η	T_{em}	W_{loss} based on T_{em} and ω	T_{op}	% error	Updated efficiency
1	92%	11.5597	292.8832	11.8289	-2.33	93%
2	93%	11.6853	294.7428	11.8242	-1.19	94%
3	94%	11.8110	296.6024	11.8195	-0.07	

The convergence of percentage error to less than 1% is denoted by grey cell in Table 1. So the value of maximum shift torque at 3800 rpm with a pulse power of 5 kW from the battery is 11.811 Nm.

5.3 Speed synchronization using electric motor

In order to do the speed synchronization by electric motor the inertia J_{em_ext} must be taken from an initial speed ω_{em_i} to a final speed ω_{em_f} as defined by equations 6 and 7 respectively. The inertia J_{em_ext} is the sum of electric motor inertia and inertia of complete input shaft and idler gears reflected on the electric motor. Since electric motor torque T_{em} is not a constant but calculated for each value of electric motor shaft speed ω_{em_now}, the resulting speed synchronization trajectory is calculated by the algorithm shown in Figure 18. ω_{em_now} is initialized with ω_{em_i} and the conditional loop in algorithm will run until ω_{em_now} is equal to ω_{em_f}. ω_{em_now} is updated in every iteration based on T_{em} as shown by the ''Update'' block by the corresponding equation

$$\omega_{em\_now}(t + \Delta t) = (sign\ \Delta\omega_{em}) \times (T_{em}(t) \div J_{em\_ext}) * \Delta t + \omega_{em\_now}(t) \tag{23}$$

where Δt is a small time step used in this discretized version of the shaft speed dynamics. Once ω_{em_now} is equal to ω_{em_f}, the synchronization time using electric motor is

$$t_{se} = N \times \Delta t \tag{24}$$

where N is the total number of iterations required for ω_{em_now} in the algorithm to reach ω_{em_f} from ω_{em_i}.

5.4 Decreasing the calculation time

The calculation time depends on number of iterations in Figure 18 and Figure 17.
As shown in Figure 18, in every iteration of the algorithm ''Torque Calculation'' is called. The calculation time increases if high number of iterations are needed for percentage error to converge to less than 1% as shown in Figure 17. To decrease calculation time, the final efficiency η_{upd} that resulted in percentage error to be less than 1% in the nth iteration of the loop in Figure 18 is also output from ''Torque Calculation''. The η_{upd} is then input as initial guess of efficiency in n+1st iteration of the loop as explained in section 5.2.
This method greatly decreases the calculation time since if Δt is small the operating point of motor at nth iteration and operating point at n+1st iteration will be very close, so the efficiency values of these two points will be close as well. Also the number of iterations in the loop shown in Figure 18 can also be decreased, if Δt is increased. If battery power available is low, it implies that values of torque will be low as well, meaning that the iterations required for ω_{em_now} to be equal to ω_{em_f} will be high. In that case Δt can be increased to decrease the number of iterations.

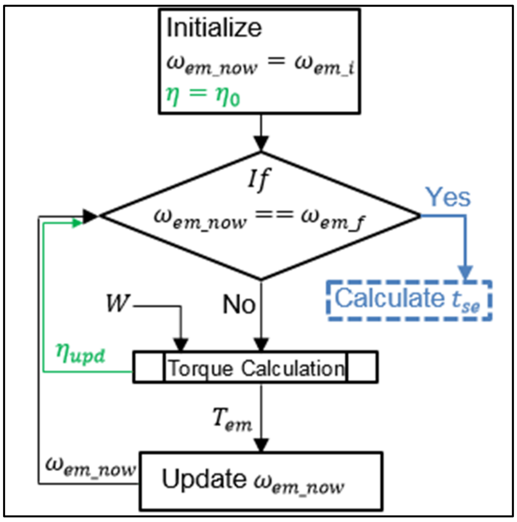

Figure 18 Algorithm to calculate speed synchronization trajectory using electric motor only

5.5 Prediction of speed synchronization trajectory with electric motor

When the calculation time is decreased by methods described in section 5.4, the speed synchronization trajectory if only electric motor is used, can be predicted before the vehicle has reached the shift velocity. Equation 1 through 7, can be used to calculate ω_{em_i}

and ω_{em_f}, then using the available battery power in combination with Figure 18, and equation 24, the profile of speed synchronization from ω_{em_i} to ω_{em_f} and the duration of speed synchronization t_{se} can be predicted. The speed synchronization trajectory vs normalized time, for a 6-2 downshift when accelerator pedal is fully pressed is shown in Figure 19. It can be seen that the speed synchronization with 40 kW available battery power represented by magenta curve is quick, 88% of the typical speed synchronization time for a DCT, but for the same shift when done with available power 5 kW represented by the black curve, synchronization time is longer and is 772% more than the typical speed synchronization time. This is of course expected since when power available in battery is 40 kW, motor torque would be in 110-30 Nm range, but when power available from battery is only 5 kW motor torque would be in 15-3 Nm, for these particular motor shaft speeds as shown in Figure 20.

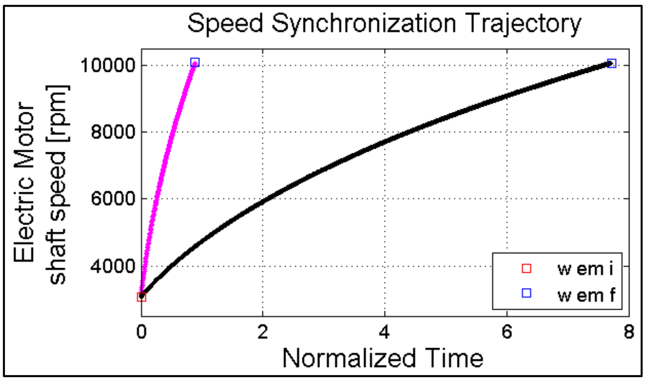

Figure 19 Speed synchronization trajectory using electric motor only for 6-2 downshift at full pedal with 40 kW (magenta) and 5 kW (black) available battery power

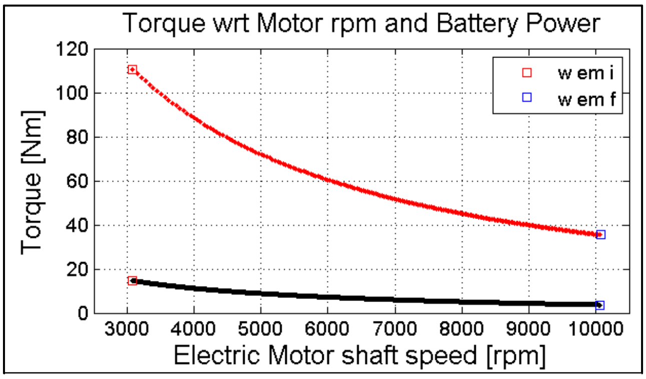

Figure 20 Torque available for shift with 40 kW (red) and 5 kW (black) available battery power

6 Supervisory Control

Based on the predicted speed synchronization trajectories by using only synchronizer, shown in Figure 15 in section 4.4, and speed synchronization trajectories using only electric motor, shown Figure 19 in section 5.5, the option that results in minimum synchronization time can be selected by following algorithm.

$$if\ t_{se} < t_s \xrightarrow[then]{} Use\ electric\ motor\ only \tag{25}$$

$$if\ t_{se} > t_s\ AND\ \ \omega_{em\_i} == \omega_{em\_iSL} \xrightarrow[then]{} Use\ synchronizer\ only \tag{26}$$

$$if\ t_{se} > t_s\ AND\ \ \omega_{em\_i}\sim = \omega_{em\_iSL} \xrightarrow[then]{} Use\ both\ electric\ motor\ and\ synchronizer \tag{27}$$

where time t_{se} is the result from equation 24 and t_s is the result from equation 14, and motor shaft speeds ω_{em_i} and ω_{em_iSL} are the results from equation 6 and equation 22 respectively.

6.1 Application of Supervisory Control on different shifts

Speed synchronization trajectories vs normalized time for a 4-6 upshift with accelerator pedal fully pressed are shown in Figure 21. It can be seen that speed synchronization time for this particular shift using electric motor only with 40 kW available battery power as represented by the magenta curve is 28% of the typical speed synchronization time. Speed

synchronization time when only synchronizer is used is 94% of the typical speed synchronization time as shown by the blue curve. So according to condition 25, only electric motor should be used for speed synchronization if available battery power is 40 kW.
The same shift when speed synchronization is done by electric motor only and power available in battery is 5 kW results in speed synchronization time 230% of the typical speed synchronization time as shown by the black plot in Figure 21.
Also since ω_{em_iSL} is equal to ω_{em_i} as denoted by coinciding of star and motor shaft rpm at time t=0 in Figure 21, this particular shift can be made with the synchronizer without exceeding its specific frictional work limit, as discussed in section 4.4. So if available power from battery is 5 kW, condition 26 is fulfilled, therefore only synchronizer is sufficient for speed synchronization.
It can also be stated that for this particular shift, the maximum time for speed synchronization will always be less than 94% of the typical speed synchronization time.
In Figure 22, a 6-2 downshift is shown with accelerator pedal fully pressed and with 5 kW power available in battery. It can be seen that the speed synchronization time if only electric motor is used will be 772% of the typical speed synchronization time, and speed synchronization cannot be achieved with synchronizer since ω_{em_iSL} is not equal to ω_{em_i}.

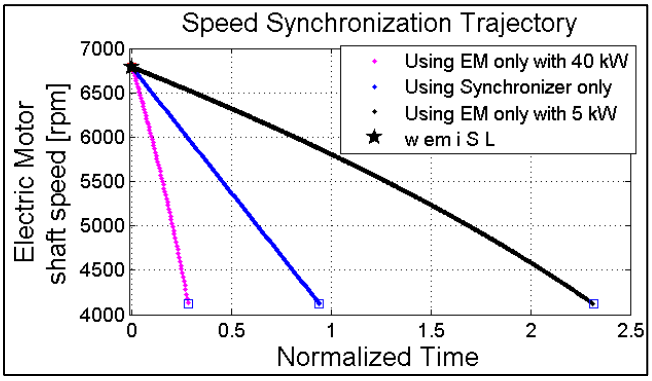

Figure 21   Speed synchronization trajectory for 4-6 Upshift with synchronizer or with electric motor with 40 kW or 5 kW available battery power

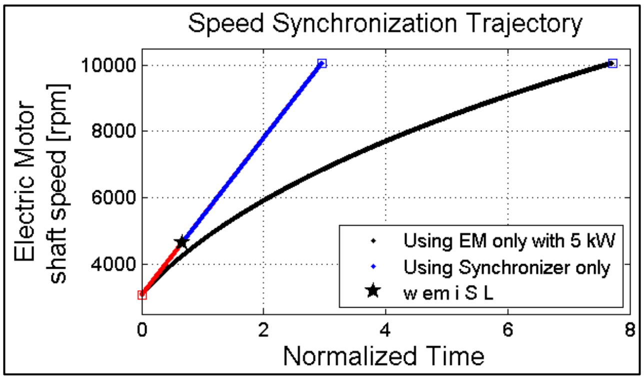

Figure 22   Speed synchronization trajectory for 6-2 Downshift with synchronizer or with electric motor with 5kW available battery power

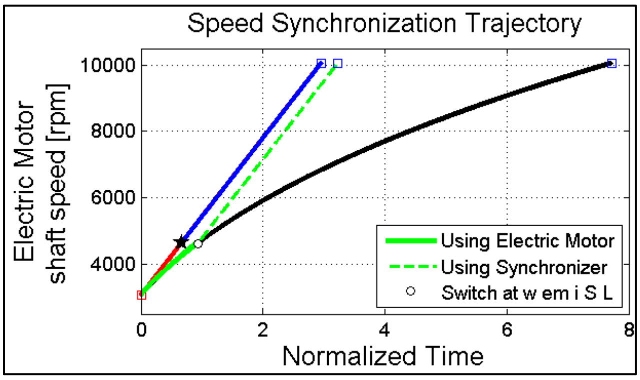

Figure 23   Proposed solution for speed synchronization when synchronizer limit is exceeded and available battery power is low

A proposed solution is shown in Figure 23, where electric motor is used to take the speed from ω_{em_i} to ω_{em_iSL} and synchronizer is used to take the speed from ω_{em_iSL} to ω_{em_f}. By using this approach the synchronizer will not exceed its specific frictional work limit and speed synchronization will be completed in 320% of the typical speed synchronization time i.e. less than half of the time if only electric motor is used.

7 Conclusions

In this paper one of the important aspects of drivability is studied i.e. minimization of speed synchronization time during torque interrupt shifts. Based on detailed simulation models of synchronizer and electric motor a prediction algorithm is designed which can predict the speed synchronization time for any shift before it is ordered by the high level controller. Some shifts exceed the specific frictional work limit of synchronizer and if performed will decrease its life. The speed points that bring such shifts within the before mentioned limit are also calculated by the prediction algorithm.

The effects of available battery power on electric motor performance during speed synchronization is also included in the prediction algorithm.

Based on the results of prediction algorithm a supervisory controller is proposed that will communicate between speed controller of electric motor and position controller of synchronizer to minimize the speed synchronization time.

It is concluded that

1. If the available battery power is high, then speed synchronization is done by using only electric motor.
2. If the battery power is low and the speed synchronization can be done without exceeding the specific frictional work limit of synchronizer, then only synchronizer is used.
3. If the battery power is low and the shift cannot be done without exceeding the specific frictional work limit of synchronizer, then electric motor is used until the speed is at a certain point and from there on synchronizer is used for speed synchronization.

8 References

[1] S. T. Razzacki, "Synchronizer Design: A Mathematical and Dimensional Treatise," in *2004 SAE World Congress*, Detroit, 2004.

[2] H. Naunheimer, B. Bertsche, J. Ryborz and W. Novak, "Gearshifting Mechanisms," in *Automotive Transmissions: Fundamentals, Selection, Design and Application Second Edition*, Springer, 2011, pp. 310-334.

[3] C.-Y. Tseng and C.-H. Yu, "Advanced shifting control of synchronizer mechanisms for clutchless automatic manual transmission in an electric vehicle," *Mechanism and Machine Theory, Elsevier,* pp. 37-56, 2015.

[4] "Documentation for Complete synchronizer with state machine," in *Powertrain library Help Documentation*, LMS Imagine AMESim.